

Elucidating Slit-Independent Mechanisms of Robo Receptors Regulating Neural Circuit
Formation and Head Morphogenesis in *C. elegans*

by

Chia-Hui Chen

Department of Neurobiology
Duke University

Date: _____

Approved:

Dong Yan, Supervisor

Anne West

Vann Bennett

Jeremy Kay

Scott Soderling

Dissertation submitted in partial fulfillment of
the requirements for the degree of Master of Science in the Department of
Neurobiology in the Graduate School
of Duke University

2018

ABSTRACT

Elucidating Slit-independent mechanisms of Robo receptors regulating neural circuit
formation and head morphogenesis in *C. elegans*

by

Chia-Hui Chen

Department of Neurobiology
Duke University

Date: _____

Approved:

Dong Yan, Supervisor

Anne West

Vann Bennett

Jeremy Kay

Scott Soderling

An abstract of a dissertation submitted in partial
fulfillment of the requirements for the degree
of Master of Science in the Department of
Neurobiology in the Graduate School of
Duke University

2018

Copyright by
Chia-Hui Chen
2018

Abstract

Neurons communicate through chemical synapses, and axon pathfinding is critical for correct synaptic pairing and therefore normal functions. With great effort put into understanding this intricate and precise process, many pathways underlying axon pathfinding have been revealed including the Slit-Robo pathway. The Slit-Robo pathway has been shown to be integral to multiple steps of the neural development. Interestingly, *C. elegans* mutants of Robo, but not Slit, exhibit severe epithelial phenotypes, indicating Slit-independent functions of Robo. Using the RME circuit as a model, we show that neuronal expression of the extracellular domain (ECD) of SAX-3, the only *C. elegans* Robo homolog, and RME expression of full-length SAX-3 rescued the circuit formation defects, indicating a ligand-like function of SAX-3 ECD. Our imaging studies reveal nuclear signals of SAX-3 during the critical period of RME circuit development. Results from both genetic and biochemical analysis support that SAX-3 intracellular domain (ICD) is cleaved and regulates RME circuit formation. In addition, neuronal expression of SAX-3 ECD is sufficient to rescue the epithelial phenotype, further suggesting a non-receptor role of SAX-3. In this study, we have identified the ectodomain of Robo receptors regulating epithelial development in the *C. elegans*. We have provided a potential mechanism to the long-known Slit-independent Robo phenotypes: the cleavage of the Robo ICD. In summary, our work increases the understanding of a conserved protein family which plays central roles in many biological processes.

Contents

Abstract.....	iv
List of Tables.....	vii
List of Figures.....	viii
Acknowledgements	ix
Chapter 1. Introduction	1
1.1 Introduction to Robo receptors.....	1
1.1.1 Molecular structures of Robo receptors.....	1
1.1.2 Slit is the conserved ligand for Robo receptors	2
1.1.3 Functions of the Slit-Robo pathway.....	4
1.1.4 Functions of the Slit-independent Robo pathway	6
Chapter 2. Cleavage and Nuclear Translocation as a Potential Mechanism Underlying a Slit-independent Robo Pathway.....	7
2.1 Introduction.....	7
2.2 Material and Methods	9
2.2.1 Strain information.....	9
2.2.2 Phenotyping of RME Circuit Defects	9
2.2.3 DNA Constructs and Expression.....	9
2.2.4 Confocal Imaging of Embryos and L1 larva.....	10
2.2.5 Protein Analysis	10
2.3 Results	11
2.3.1 A Slit-independent Robo pathway regulates RME circuit formation.....	11
2.3.2 Slit-independent Nuclear Signals of SAX-3 during Critical Period of RME Circuit Formation	16

2.3.3 The Slit-independent cleavage of SAX-3 at both extracellular and intracellular regions.....	20
2.3.4 SAX-3/Robo Extracellular and Intracellular Domains Have Different Functions	22
Chapter 3. Conclusion and Future Directions	26
References.....	29

List of Tables

Table 1. Summarized Phenotyping Results of Rescuing Experiments with One Transgene	24
Table 2. Summarized Phenotyping Results of Rescuing Experiments with Two Transgene	25

List of Figures

Figure 1. Sequence Alignment of homologs of <i>sax-3</i>	14
Figure 2. RME circuit formation is mediated by Robo in a Slit-independent fashion.....	15
Figure 3. Slit-independent Nuclear Signals of SAX-3 from Embryonic to L1 Stages	17
Figure 4. Quantification of Nuclear Signals of SAX-3::GFP Embryos.....	19
Figure 5. SAX-3 Cleavage Is Slit-independent and Is Cleaved in Both the Extracellular and Intracellular Regions	21

Acknowledgements

I would like to express my gratitude to Dr. Dong Yan. When things did not work out for me after my five rotations, Dr. Yan kindly invited me to join his lab, which meant a lot to me. A heartfelt thank-you must be said to my thesis committee as well. They used their valuable time helping me along the way and made me feel supported even in the worst time. I want to thank Dr. Anne West for spending hours talking with me. Her guidance and support are very important during my transition from Ph.D. to Master. Miss Carla Sturdivant helped me a lot with technical and emotional supports. She sent me an e-mail just to make sure that I don't feel stressed overnight and I cannot thank her enough for her constant care and support. I am blessed with both Carla and Carol, our retired DGSA of the CMB program, who helped me navigating through the difficult time during my first two years. I am eternally grateful to Dr. Hsou-min Li at the Academia Sinica of Taiwan, who believed and supported me. Without her help, I won't have the chance to study at Duke. I want to thank members of the Yan lab, who have been great companies. Dr. Lingfeng Meng is a great collaborator and has helped me tremendously on my research. Dr. Lezi E is a great friend and has offered me advice both professionally and personally. I thank my friends in the lab who have worked with me for countless hours: Sophia, Yuki, Clara and those without names. Miaomiao and Eva are my dearest friends during my journey at Duke and have been an integral part of my life here. I have met many wonderful people and I will name a few of them for their friendships are invaluable to me: Baoxia, Paige Dexter, Paige Vinson, Claudia and Jims, Chi-Fang, and Ming-Feng. Finally, I thank my family for their unconditional support and love.

Chapter 1. Introduction

1.1 Introduction to Robo receptors

1.1.1 Molecular structures of Robo receptors

Robo is discovered in a genetic screen affecting growth cone guidance in *Drosophila* [1]. Robo describes the original phenotype of “roundabout” axons. Later, the *C. elegans* Robo homolog, *sax-3*, is identified also in a genetic screen for factors affecting axons of sensory neurons [2]. Robo is well conserved from *C. elegans* to humans with similar domain organization in the ectodomain. As members of the immunoglobulin superfamily, most Robo receptors contains 5 immunoglobulin (Ig) domains and 3 fibronectin type III (FN3) repeats in the ectodomain. Robo receptors have a single transmembrane (TM) domain and a less well conserved intracellular region. Four small conserved cytoplasmic (CC) motifs have been identified but are not universally conserved in Robo family members [3]. The number of Robo receptors seem to increase along the evolution: In *C. elegans*, *sax-3* is the only Robo homolog; *Drosophila* has three Robo receptors, and in vertebrates (zebrafish, mouse, human), the Robo family consists of four members: Robo1,2, 3, 4. Expression of all Robo receptors except for Robo4 can be found in the nervous system. Robo4 expression is specific in the vascular system, functioning in endothelial migration [4]. Structurally, Robo4 is also different from other Robo receptors as it has less Ig domains and FN3 repeats. In the case of Human ROBO4, there are two of each domain (Ig domains and FN3 repeats).

1.1.2 Slit is the conserved ligand for Robo receptors

Several years after the discovery of Robo, Slit proteins were identified to be their ligands in both *Drosophila* and mice [5, 6]. In the *Drosophila*, the surface expression of Robo is negatively regulated by *comm*, which keeps expressed Robo proteins in the ER. The fact that strong *comm* gain-of-function phenotypes are similar with *slit* loss-of-function phenotypes intrigued Kidd and colleagues to investigate the role of *slit* in axon guidance. Slit was shown to be expressed in the midline glia of *Drosophila* using immunoelectron microscopy [7]. In rats, Slit proteins also express in the midline of the spinal cord, the floor plate. Equilibrium binding tests using recombinant Slit and Robo proteins demonstrated that Slit interacts with Robo with the similar affinity between Netrin and its receptors [5]. Furthermore, hSlit2 was able to repel motor axon growth of the explant spinal cord. Taken together, it was concluded that slit proteins are conserved ligands for Robo receptors. Slits are secreted protein with a signaling peptide at the N terminal, 4 leucine rich repeats (LRR), 7 to 9 epidermal growth factor (EGF) repeats, a LNS (laminin, neurexin, slit) spacer and a cysteine knot at the C terminal [8]. Slit interacts with Robo receptors through its second LRR (also termed D2) binding two the first two Ig domains of Robo receptors [9]. Slits are cleaved into two fragments with the larger N-fragment interacting with Robo receptors and the smaller C fragment is recently identified as a ligand of plexinA1 [10].

Downstream signaling of the Slit-Robo pathway

Similar as other guidance receptors, downstream signaling of Slit-Robo regulates the cytoskeleton, mainly through regulation of Rho family small GTPases. A group of GAP proteins associating with Robo receptors are termed srGAP (slit-robo Rho GTPase

activating protein), which is proposed as the link between Slit-Robo to cytoskeleton [11]. The srGAP family, like the Slit-Robo pathway, is extremely well conserved with one member in the nematode and 3 members in humans, suggesting comparable downstream signaling between *C. elegans* and human Slit-Robo pathways. It is known that srGAP1 associates with Robo receptors at proline-rich CC2 or CC3 domains via its SH3 domain [12]. There appear to be specificity between srGAP and Rho GTPase as evidence suggests that srGAP1 and srGAP3 predominantly regulates Cdc42 and Rac1 activity respectively [11, 13, 14]. Samocovlis's group has identified a Robo associating Rac/Cdc42 GAP family termed Vilse in *Drosophila*. The Vilse family is conserved in vertebrates but lack a homolog in *C. elegans* [15].

The Abelson (Abl) tyrosine kinase and its substrate Enabled (Ena) regulate motor axon guidance under a receptor phosphatase Dlar (*Drosophila* liprin alpha receptor) [16]. Interestingly, both Abl and Ena physically interacts with the cytoplasmic region of Robo receptors, similar as with Dlar. Ena transduces signals from Robo and promote inhibition as Robo with mutations of Ena binding site has impaired ability to rescue Robo loss of function phenotypes. At the other hand, a Y-F mutation of a phosphorylation site (a tyrosine at juxtamembrane region of Robo) of Abl creates a hyperactive Robo, suggesting that Abl antagonizes Robo function through direct phosphorylation. As a result, activation of Robo receptors have two opposing effects [17]. However, Abl does not always antagonize repulsion. Robo activation inhibits the calcium dependent cell-cell adhesion mediated by N-cadherin. Slit, Robo, N-cadherin and Abl form a protein complex to mediate this process [18]. Through phosphorylation of β -catenin associated

with N-cadherin, Abl promotes dissociation of β -catenin from N-cadherin, which causes a decrease of adhesion mediated by N-cadherin [19].

1.1.3 Functions of the Slit-Robo pathway

Midline guidance

Identified as guidance receptors, Robo receptors are most well known for their role in midline guidance, which is well described in *Drosophila*. Robo expresses in commissural axon but are not membrane targeted before the axon crosses midline. Instead of being presented on the plasma membrane, Robo proteins are retained in the Golgi network. This process is mediated by commissureless (comm), which expresses before commissural axon crossing the midline [3]. In the vertebrates, no comm homologs have been identified and a different molecular strategy is utilized to solve the same problem: repulsion only after crossing. In the mice, Robo3 has been shown to prevent premature sensibility of Slit [20]. Although the underlying molecular mechanism is still unclear, the expression pattern of Robo3 supports this hypothesis as after midline crossing, Robo3 expression is drastically downregulated [21]. Sequence analysis of Robo3 revealed amino acid substitutions at binding region of Slits, which supports that Robo3 has different functions as it does not bind Slit with high affinity [22]. This down regulation of Robo3 is later explained by different isoforms of Robo3 through alternative splicing where Robo3.1 silences Slit-mediated repulsion but Robo3.2 does not [23].

In the nervous system

The Slit-Robo pathway participates multiple steps of neural development starting from neural progenitor cell regulation [24]. Most obviously, they are important in axon pathfinding in other animals including zebrafish [25], *Xenopus* [26] and mice [27]. In

humans, mutations of Robo genes also disrupt axon pathways. Mutation of the human ROBO3 is linked to a rare genetic disease: horizontal gaze palsy with progressive scoliosis [28]. In addition to axon pathfinding, Slit-Robo interactions also mediate axon fasciculation in *Drosophila* and mice [29, 30]. Both axon pathfinding and migration requires cytoskeletal regulation by extracellular guidance cues. Therefore, it is not surprising that the Slit-Robo pathway also function in neuronal migration in many areas of the brain [31, 32]. Finally, the Slit-Robo pathway also regulates dendrite development in mice. Mutations of Ena proteins, which is downstream of Slit-Robo signaling, also disturbs this process and provide a possible underlying molecular mechanism [33].

Outside the nervous system

Like many other axon guidance pathways, the Slit-Robo pathway is versatile, and functions in many biological processes. The ability to mediate cytoskeletal regulation makes Slit-Robo pathway an obvious candidate for position-related biological processes, which are key in morphogenesis. In kidney development, the Slit2-Robo2 interaction ensures a single induction site, preventing extra ureteric buds [34]. Mutations of Robo receptors in mice leads to mispositioning of the stomach into the thoracic cavity [35]. The Slit-Robo pathway also regulates the migration of cardiac precursor cells and hence the development of the heart [36]. Cancer cells, specifically glioblastoma cells, also utilize Slit-Robo interactions as an invasion mechanism [37].

In addition to conveying positional information, Slit-Robo interactions also regulate physiological states of cells, which controls several specific cellular identifies. In *Drosophila*, the cell fate decisions of adult intestinal stem cells are regulated by the Slit-Robo pathway [38]. Local secretion of Slit proteins regulates the survival of pancreatic

beta cells by suppressing apoptosis and ER stress [39]. The Slit-Robo pathway has been implicated as oncogenic as it improves survival [39], induces angiogenesis [40, 41], and promotes metastasis [42]. However, Slit-Robo interactions can suppress carcinogenesis as well [43]. Effects of Slit-Robo interactions is probably determined by intricate environmental cues including the cell type, oncogenic mutations, and nutrient conditions.

1.1.4 Functions of the Slit-independent Robo pathway

Slit and Robo are essentially two inseparable entities in all researches of Robo receptors. However, phenotypic difference between *slt-1* and *sax-3* mutants in *C. elegans*, where Robo and Slit both have only one homolog, presents a direct and strong line of evidence indicating Slit-independent functions of Robo receptors. Direct phenotypic comparison in higher animals is rarely conclusive as there are multiple members in Slit and Robo families. Nonetheless, there is still evidence showing possible Slit-independent Robo functions in *Drosophila* [44], zebrafish [25] and mice [45].

One of the possible molecular mechanisms underlying Slit-independent Robo functions is novel ligands of Robo receptors, which is being avidly explored. Recently, the Jaworski group has identified Nell2 as a ligand for Robo3, which does not bind Slit at high affinity [46]. Robo receptors contain multiple Ig domains, which have been shown to mediate homophilic interactions in Ig containing proteins like NCAM (neural cell adhesion molecule) [47] and L1 [48]. *In vitro* evidence has suggested that Robo1, Robo2 and Robo3 interacts both homophilically and heterophilically [49, 50]. However, no *in vivo* evidence of homophilic interactions between Robo receptors has been published to this date.

Chapter 2. Cleavage and Nuclear Translocation as a Potential Mechanism Underlying a Slit-independent Robo Pathway

2.1 Introduction

In the *C. elegans*, which expresses only one homolog of Slit and Robo, phenotypic differences between *slt-1* and *sax-3* mutants are direct indications of functional differences between the two genes. The most obvious example is probably the head morphology. About 20% of *sax-3* mutants exhibit deformed head while head morphology of *slt-1* mutants is normal. For axon guidance, while mutation of *slt-1* produces similar phenotypes in PLM ventral guidance, it does not affect the axon of amphid sensory neuron AWB [51]. Evidence supporting Slit-independent Robo functions is reported in other organisms. In *Drosophila*, one of the phenotypes of *robo2* mutants is misprojection of dorsal cluster sensory axons. However, Robo2 is not expressed on sensory axons but on their normal growth substrate. This suggests that Robo2 regulates dorsal cluster sensory axons in a Slit-independent fashion [44]. Although it is known that Robo have Slit-independent functions, it has been hard to study due to the complexity created by multiple Robo and Slit proteins and their importance in general development. *C. elegans* offers an excellent environment to study Slit-independent Robo functions because it circumvents both major difficulties: there is only one Slit and Robo homolog and mutants of either gene is completely lethal.

Signaling of guidance receptors have been studied avidly for decades and proteolytic modification of either ligands or guidance receptor themselves is one interesting regulation mechanism. Proteolytic modification is common in regulating

cellular events. Metabolic enzymes are often activated by specific cleavages [52], which allows stringent regulation of their activities. Many guidance receptors also utilize proteolytic modification as a signaling mechanism. Ephrin and their receptors are both membrane proteins, when binding with each other, they mediate canonic bidirectional signaling. Their interaction usually has inhibitory effects, causing axon retraction, which leaves a question about how the high affinity ligand-receptor is dissociated since they are both membrane targeted. Hattori and colleagues have found ephrin A2 is cleavage when bound with its receptor and uncleavable mutant of ephrin A2 delays axon retraction in transfected cells [53]. Slit is cleaved and into a larger N fragment, which binds Robo receptors and mediate Slit-Robo signaling, and a smaller C fragment which is the ligand for PlexinA1 [10]. Cleavage of Netrin receptor DCC is required in motor axon guidance in mice [54]. Moreover, the abovementioned cleavage of DCC triggers intramembrane cleavage, causing intracellular domain (ICD) shedding [55]. A more recent study confers the transcriptional activity of DCC ICD, which is required in commissural axon guidance [56]. In *Drosophila*, it is reported that cleavage of Robo by Kuzbanian, an ADAM family metalloprotease, in the extracellular region is essential for midline repulsion. Expression of uncleavable form of Robo in *robo* mutants does not rescue the guidance phenotype [57].

In this study, we have identified *sax-3*, the *C. elegans robo* homolog, regulates the RME circuit formation in a Slit-independent fashion. Our imaging study have identified nuclear signals of Robo::GFP during the critical stage of RME circuit development in embryos. Biochemical analysis of tagged SAX-3 protein further supports that SAX-3 is cleaved during the embryonic stage. Furthermore, we have identified a

separate and novel function of the ectodomain of SAX-3. In conclusion, our study increases our understanding of an important and complex signaling molecule.

2.2 Material and Methods

2.2.1 Strain information

Wild-type animals are N2 Bristol strain. Worms are cultured on standard NGM plates at 20°C. All mutant alleles are ordered from the Caenorhabditis Genetics Center with the exceptions as follows: two *sax-3 lf* (loss of function) alleles used in the study, *ju1119* and *yad10*, are isolated in our lab from a standard EMS mutagenesis screen. We use *yadls76 (Punc-25::gfp)* as the marker to visualize the morphology of RME neurons.

2.2.2 Phenotyping of RME Circuit Defects

Animals are categorized into “normal” and “defected” with the definition of defected is the abnormal anterior axons. Presented percentages are number of defected animals/ total animals. Animals are picked at L4 stage and quantified a day later when they are 1-day young adults. Worms are paralyzed in 1% 1-phenoxy-2-propanol (TCI America, Potland, OR) in ddH₂O and observed under 10X objective of Zeiss Axion Imager 2 microscope equipped with Chroma HQ filters. Each strain is quantified three times and statistically analyzed by one-way ANOVA.

2.2.3 DNA Constructs and Expression

Expression vectors are constructed using the Gateway technology (Invitrogen). Transgenic animals are generated following standard microinjection procedures. Expression plasmids are injected at the concentration of 50ng/μl in general. We use *Pmyo-2::mcherry* or *Pttx-3::rfp* as co-injection markers.

2.2.4 Confocal Imaging of Embryos and L1 larva

To visualize the subcellular location of SAX-3 during embryonic stages, we have generated a strain expressing *Punc-33::sax-3::gfp* (NYL1757). Embryos and L1 larva are put onto 5% agar pads in 1% 1-phenoxy-2-propanol (TCI America, Potland, OR) in ddH₂O. Images are acquired with a Zeiss LSM700 confocal microscope using a Plan-Apochroma 100x/1.4 objective. Z-stack images are taken for quantification of nuclear signals. For quantification, DIC images is checked for each round GFP signal to make sure it is nucleus. One quantification example can is presented in Figure 4.

2.2.5 Protein Analysis

To analyze the cleavage events of SAX-3, we generated a transgenic strain (NYL1426) expressing *Punc-33::sax-3::HA*. At least 20 animals are picked unto a new plate and cultured until freshly starved. Worms are washed from the plate gently with M9 buffer to minimize the number of eggs that are already laid. Worms are washed three times with M9 buffer in 15mL conical tubes and treated with death buffer (250 mM NaOH, 20% Bleach) at RT with rotation until all worms are dissolved. Eggs are washed three times with M9 buffer and lysed with LDS non-reducing sample buffer (Thermo Scientific). For time course experiments, washed eggs are kept in M9 buffer and rotated at RT and lysed at specific time points. The sample are frozen in the -80°C freezer for at least 16hrs. The egg shell is broken using 10 freeze-thaw cycles in dry ice bath (with 100% EtOH). In each cycle, samples are frozen for 5 minutes and thawed in 37°C water bath for 5 minutes. Samples are then added 5% 2-mercaptoethanol, boiled at 99°C using a PCR machine for 20 minutes before loading. Samples are resolved using 4-20% gradient SDS-PAGE gels (Bio-Rad) and transferred onto nitrocellulose membranes.

Blots are probed using Anti-HA antibodies (Sigma H6908, Thermo-Fischer 26183) and HRP-conjugated secondary antibodies (Bio-Rad 170-5046 and 170-6516). We use Supersignal West Femto Maximum Sensitivity Substrate (Thermo-Fischer) to visualize the signal.

2.3 Results

2.3.1 A Slit-independent Robo pathway regulates RME circuit formation

In an unbiased genetic screen for factors affecting RME circuit formation, we uncovered two novel alleles of *sax-3* (*ju1119* and *yad10*), a gene encoding the only Robo receptor in *C. elegans*, with displacement of RME cell bodies and axons. In control animals, four RME neurons (RMED, RMEV, RMEL and RMER) are evenly spaced along the nerve ring with their axons bundled into the nerve ring, and RMED and RMEV each develops a posterior neurite along the dorsal/ventral cord, respectively. In *sax-3* mutants, while positions of RMED and RMEV and their posterior neurites are not changed, RMEL and RMER are close to the dorsal side and stay together with RMED. The displacement of RMEL/R cell bodies can be readily observed in the late comma stage and maintains through adult stages (Fig 2A, 2B). Axons of RME neurons often grow anteriorly towards the tip of head instead of bundled into the nerve ring in *sax-3* mutants.

Sequence analysis of mutant alleles showing the *ju1119* allele has a point mutation (G to A) in exon 5, causing an amino substitution (G376E) at the fourth Ig domain. The *yad10* allele has Both newly isolated *sax-3* alleles (*ju1119*,

yad10) and a previously isolated null allele of *sax-3(ky123)* show similar RME circuit defects (Fig.2B). In addition, *ju1119* and *yad10* have similar head morphogenesis defects and embryonic lethality as those in *ky123*. The RME defects can be rescued by expressing *sax-3* cDNA under a pan-neural promoter. When expressed in body wall muscle and only GABAergic neurons including RME neurons, *sax-3* cDNA does not rescue the RME defects. These results suggested that both *ju1119* and *yad10* are likely null alleles of *sax-3*. Also, *sax-3* does not act cell-autonomously in mediating the RME circuit formation.

Next, we asked that if RME circuit formation is regulated by *slt-1*, the ligand of SAX-3/Robo in *C. elegans*. We examined two *slt-1* null alleles and observed weak RME defects in less than 5% of animals, suggesting that *slt-1* is not the major player mediating RME circuit formation. In *C. elegans*, *eva-1* encodes a receptor functioning in the Slit pathway in axon guidance. We tested *eva-1(lf)* animals and did not observe any RME defects. Previous studies have shown that Slit/Robo pathway interacts with the Netrin pathway in regulating axon guidance. We tested the function of the Netrin pathway in RME circuit formation and did not observe any RME defects in *unc-6* (the only Netrin homolog in *C. elegans*), *unc-5* and *unc-40* (DCC homolog) mutants. Since *sax-3* mutants display defects of head morphogenesis, one may argue that RME defects could be a result of abnormal head morphology. To rule out this possibility, we tested *vab-1(lf)* mutants, which exhibited similar defects of head morphogenesis as seen in *sax-*

3(lf) mutants. As shown in Fig.2C. *vab-1(lf)* mutants did not have any *sax-3(lf)*-like RME defects, supporting that defects of head morphogenesis are not the cause of the RME defects. Based on these results, we conclude that *sax-3* regulates RME circuit formation through a Slit-independent mechanism.

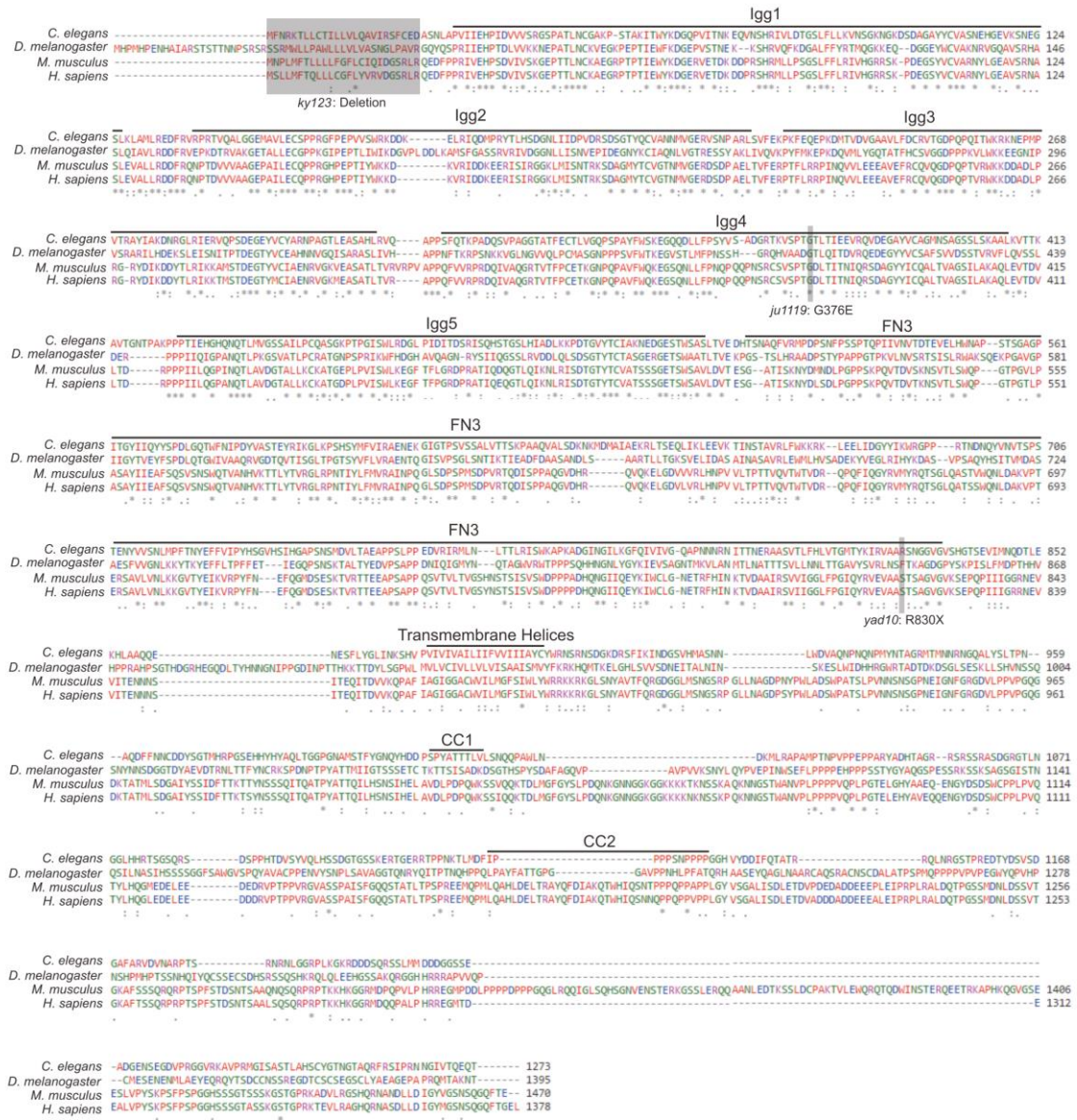


Figure. 1 Sequence Alignment of homologs of sax-3

Protein sequence are aligned using Clustal Omega (EMBL-EBI). Protein from each organism: SAX-3 (*C. elegans*); Robo2 (*Drosophila*); Robo2 (mice); Robo2b precursor (Hsman). Conserved protein domains are noted using lines above. Mutant regions of alleles used in the study are marked in grey boxes.

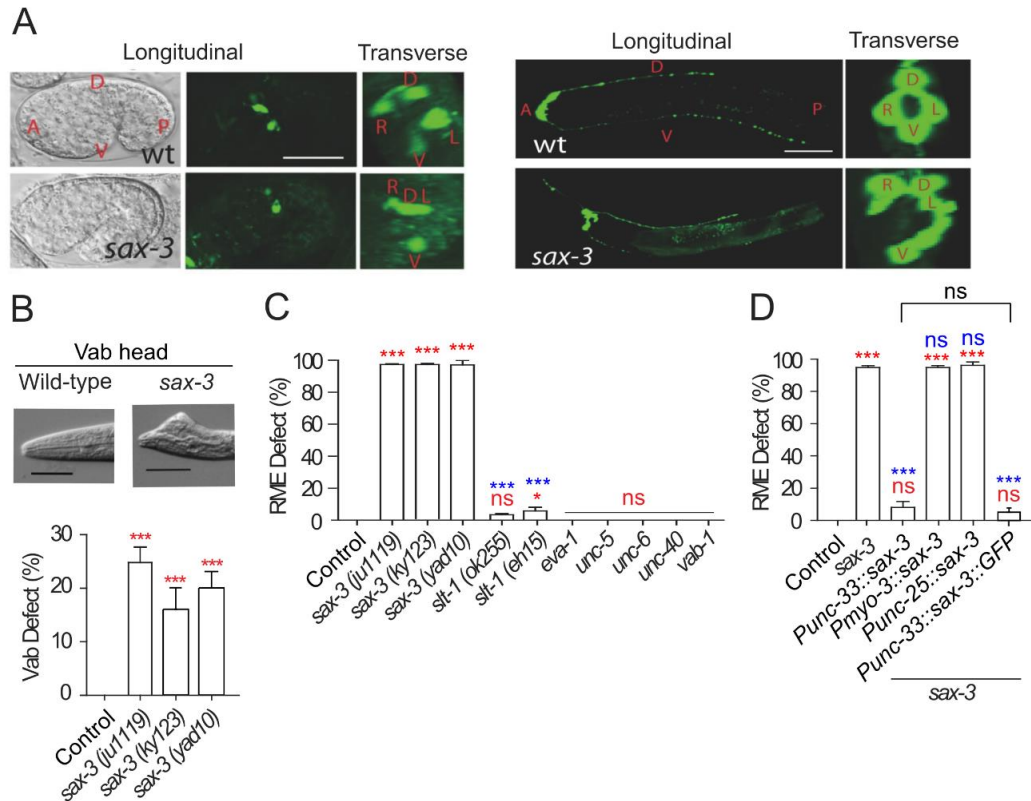


Figure. 2 RME circuit formation is mediated by Robo in a Slit-independent fashion

Phenotyping results of *sax-3* mutants. (A) Left panel: positional defects of RME neurons at the late comma stage. RMER/L neurons are closer to RMED in *sax-3* mutants compared to wildtype embryos. Right panel: RME circuit morphology in young adult animals. Abnormal cell positions and anterior axons are observed in *sax-3* mutants. Positional information is labeled in red: A: anterior; P: posterior; D: dorsal; V: ventral; L: left; R: right. (B) Head morphology of *sax-3* mutants. (C) Quantification of the RME anterior axon phenotype in Slit, *eva-1*, the Netrin pathway and *vab-1* mutants. (D) Quantification of the RME anterior axon phenotype in transgenic animals expressing *sax-3* cDNA, showing pan-neural expression of *sax-3* rescues the phenotype.

2.3.2 Slit-independent Nuclear Signals of SAX-3 during Critical Period of RME Circuit Formation

To understand the Slit-independent Robo mechanism underlying RME circuit formation. We searched for established regulatory mechanisms of Robo receptor activities. In mediating the *Drosophila* midline guidance, the subcellular localization of Robo serves as the switch to turn off the repellent effect of Slit to commissural neurons. To examine the subcellular localization of SAX-3, we generated a transgenic strain with pan-neural expression of SAX-3::GFP. The fusion protein, SAX-3::GFP, is bioactive as it rescues the RME circuit formation defects effectively as the *sax-3* cDNA when expressed under a pan-neural promoter (Fig. 2D). Since the positional defects of RMEL/R neurons can readily be observed during the late comma stage, we figure that the critical stage of RME circuit formation is at or before the late comma stage. In all embryos imaged, SAX-3::GFP localizes to the membrane as expected (Fig. 3A). Surprisingly, in addition to the membrane expression, we also found round GFP signals inside cells, reminiscent of nuclear localization. To confirm the nuclear localization, we co-expressed SAX-3::GFP and a nuclear marker (mCherryH2B). The intracellular signal of SAX-3::GFP co-localized well with mCherryH2B, supporting that SAX-3 or part of SAX-3 translocates into the nucleus during embryonic stages.

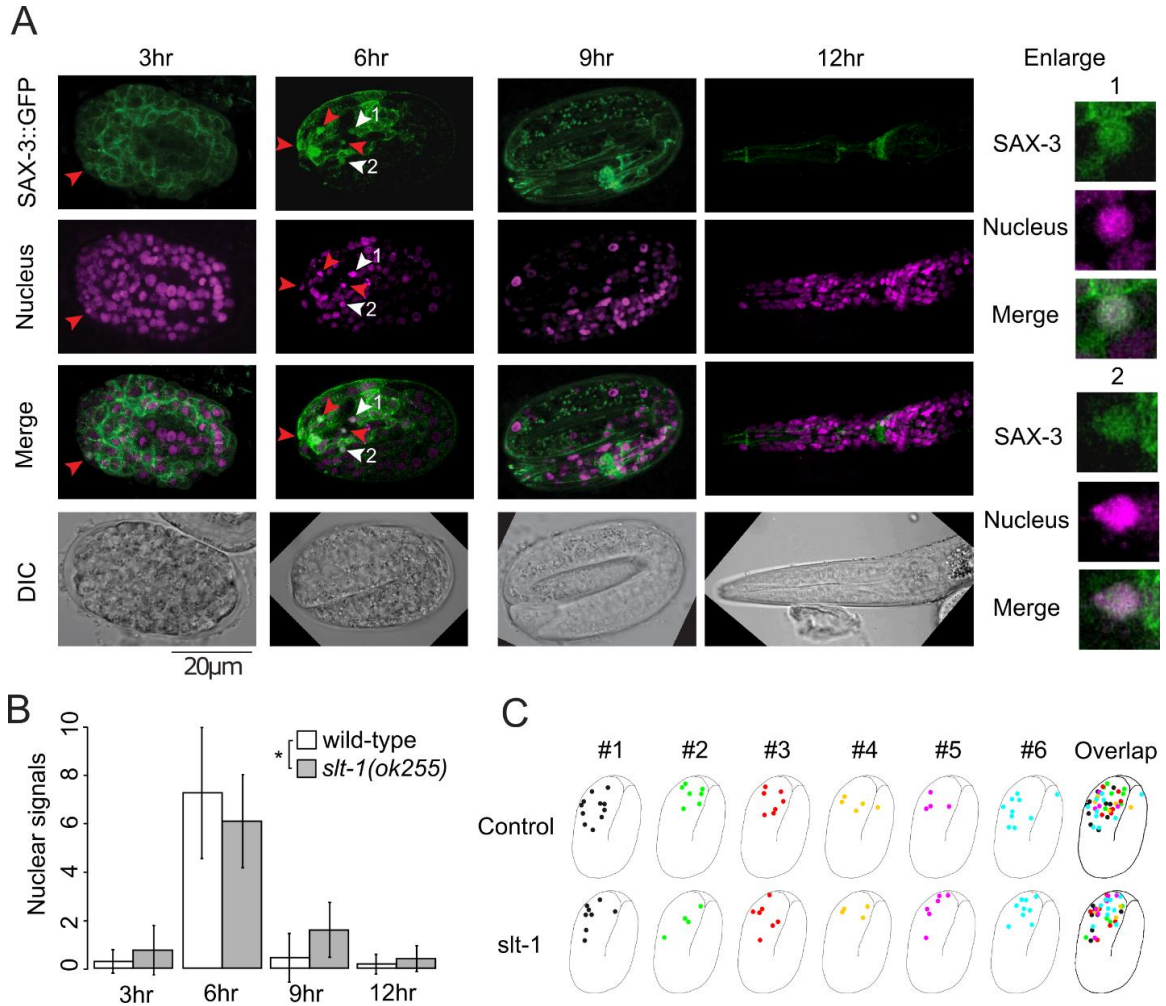


Figure. 3 Slit-independent Nuclear Signals of SAX-3 from Embryonic to L1 Stages.

Images of embryos and L1 larvae expressing SAX-3::GFP and mCherryH2B expressed under the pan-neural promoter, *Punc-33*, showing co-localization of SAX-3::GFP with the nuclear marker at early embryonic stages. Red arrowheads indicate nuclear signals. White arrowheads indicate nuclear signals with an enlarged version on the right panel. (B) Quantifications of nuclear signals of the same transgene in the *slt-1* mutant background. Wild-type and *slt-1* mutant signals are compared by one-way ANOVA, showing minor significance between two groups. (C) Localizations of nuclear signals in 6hr embryos of wild-type and *slt-1* mutant animals.

To further characterize the nuclear translocation event of SAX-3::GFP, we quantified numbers of nuclear signals at different time points during embryonic stages. The quantification showed that most nuclear signals are observed during the 6hr time point but could be observed at each time point we examined (Fig. 2B). If the nuclear localization of SAX-3 is important for the development of the RME circuit, the nuclear translocation event should not be impaired by Slit mutations. Indeed, the nuclear signal profile of SAX-3::GFP in a *slt-1 (ok255)* mutant also peaks at the 6hr time point with signals detected throughout the embryonic stages, showing that the nuclear translocation event does not require Slit. The number of nuclear signals is low in our quantification results with the peak number less than 8. We therefore asked that whether it is a specific subset of neurons that has SAX-3 nuclear translocation. To answer this question, we summarized locations of nuclear signals of five embryos and superimposed them (Fig. 2C). Results showed that, in both wild-type and *slt-1* mutant embryos, nuclear signals concentrated on the head region with sparse signals on the tail, consistent with the locations of most neurons. We found that nuclear signals are not found at similar locations in different embryos. Cell locations during the development of *C. elegans* is programmed and highly reproduceable. We therefore concluded that nuclear translocations of SAX-3 occur in many neurons. SAX-3 nuclear translocation might be transient, resulting in signals from different neurons captured in different embryos.

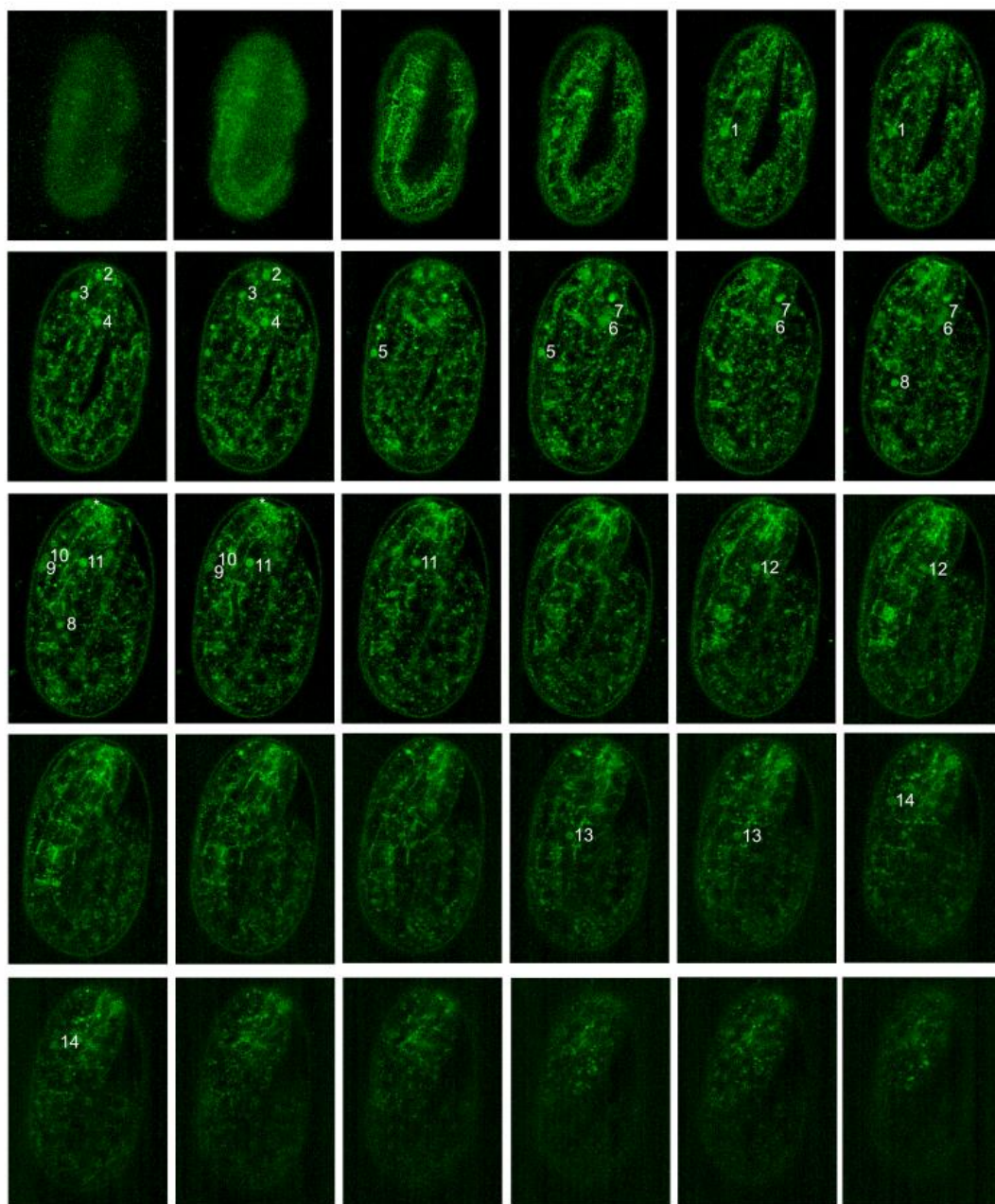


Figure. 4 Quantification of Nuclear Signals of SAX-3::GFP Embryos.

Z-stack images are taken for each embryo. Round GFP signal are found in each section and double-checked using DIC images taken together with fluorescent images to make sure the GFP signal is in the nucleus.

2.3.3 The Slit-independent cleavage of SAX-3 at both extracellular and intracellular regions

When we carried out the rescue experiments, to ensure the expression of each truncated proteins we examined the expression of those proteins by tag a GFP at their C-terminals. While confirmed the expression of all these proteins, we observed that there are clearly nuclear GFP signals in transgenes with neuronal expression of full length SAX-3::GFP functional fusion protein. More importantly, the most noticeable period with nuclear GFP signals is the same developmental stage when most of Slit-independent *sax-3* phenotypes are originated. We also found that this nuclear GFP signals seemed to be transient, as careful analyses of six embryos showed that there was little overlap of neurons with nuclear GFP signals. As summarized in Fig. 3C, it appears that many neurons transiently express nuclear GFP signals. Further experiments showed that loss-of-function in Slit did not affect the number or the timing of neurons with nuclear GFP signals. Since we fused GFP at the C-terminal of SAX-3, the nuclear GFP signals is likely caused by cleavage of the SAX-3 intercellular region. To test this idea, we collected transgene animals as different stages and analyzed the expression of SAX-3::GFP. As shown in Fig. 5A, in addition to the full length SAX-3 we observed three major cleavage products, and we named it as product 1, 2 and 3. Based on their molecular weight, the product 1 and 2 are likely generated by cleavages at the beginning and the end of FN3 repeats, respectively, and the product 3 is generated by a cleavage at the SAX-3

intracellular region. We further confirm this result using multiple transgene lines as well as different antibodies. As shown in Fig.5B, consistent as the observation in SAX-3::GFP transgenes, loss-of-function in Slit did not affect those cleavages. Interestingly, an earlier study shows that *Drosophila* Robo can be cleaved at the FN3 repeats, and this cleavage is important for Slit-dependent axon guidance. In our analyses, the product 1 is generated at the time when most of axons growth happens in *C. elegans*, and it likely play similar role as its homolog in *Drosophila*. However, the cleavage product 2 and 3 are only observed at early embryos when most of Slit-independent phenotypes are originated. Therefore, we decided to focus on our analyses on the product 2 and 3.

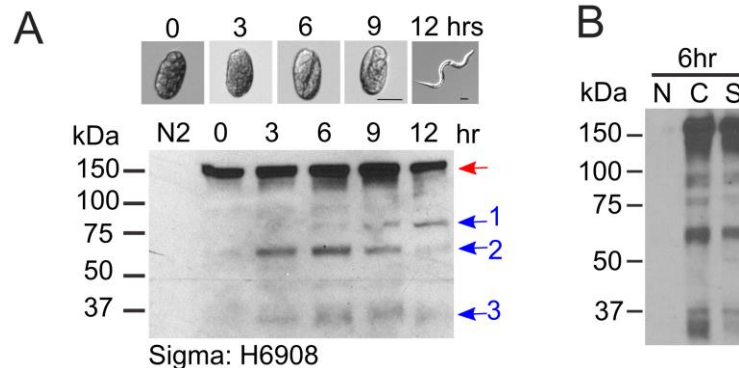


Figure. 5 SAX-3 Cleavage Is Slit-independent and Is Cleaved in Both the Extracellular and Intracellular Regions.




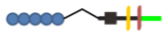







Eggs from transgenic animals expressing *Punc-33::sax-3::HA* are prepared as described. (A) SAX-3 is cleaved during critical embryonic stages of the RME circuit formation. Red arrow: the full-length SAX-3::HA protein. Blue arrows: cleavage products of SAX-3::HA. (B) Cleavage of SAX-3 is Slit-independent. N: N2. C: control. *Punc-33::sax-3::HA* expressed in the N2 background. S: *slt-1* mutant. The same extrachromosomal array of *Punc-33::sax-3::HA* crossed into *slt-1* (*ok255*) background.

2.3.4 SAX-3/Robo Extracellular and Intracellular Domains Have Different Functions

To uncover the molecular mechanism underlying the Slit-independent *sax-3* phenotypes, we decided to further examine RME and head morphogenesis (*vab* head) defects in *sax-3* mutants. We first asked that where SAX-3 functions in these two phenotypes. Consistent with previously reports, we found that expression of *sax-3* cDNA in all neurons completely rescued both RME and head morphogenesis defects in *sax-3(lf)* mutants, while expressing *sax-3* cDNA in body wall muscle or RME neurons did not show any rescue ability in either phenotypes (Fig. 2E). To further understand how SAX-3 function, we examined the rescue ability of neuronal expression of different truncated forms of SAX-3. As shown in Table 1, expression of *sax-3* lacking either Ig 1-2 or Ig 3-5 can still partially rescue *sax-3(lf)* phenotypes, while deleting FN3 repeats completely abolished its rescue ability on both phenotypes. As previously studies show that Slit directly binds with Ig1-2 domains of SAX-3 to regulate axon growth, our results further support the conclusion that a Slit-independent mechanism underlies these phenotypes. To our surprise, expression of SAX-3 without its intracellular domains can still rescue *sax-3(lf)* *vab* head phenotypes to similar a level as the full length (Table 1), while this deletion lost its rescue ability for RME circuit formation. Those observations suggest that the SAX-3 FN3 repeats are essential for all Slit-independent phenotypes, while the SAX-3 intracellular

domains are only involved in neuronal circuit formation but not head morphogenesis.

Since intracellular signaling of SAX-3 is important for RME circuit formation, we questioned whether the intracellular signaling functions cell autonomously in RME neurons. Evidence supports this hypothesis that expression of the no-rescue *sax-3* extracellular domains in all neurons together with full length *sax-3* in RME neurons rescued RME defects of two *sax-3(lf)* alleles to a similar extent as full-length *sax-3* expressed in all neurons (Table 2). These results support a model that SAX-3 in other neurons may use its extracellular domains as ligands to pass signals to the receptor SAX-3 on RME neurons to mediate normal RME circuit formation. We then asked that which extracellular domain of SAX-3 is required in the “ligand” and “receptor”. As shown in Table 1, by testing rescue ability of different truncated SAX-3, we concluded that in the SAX extracellular region FN3 repeats is essential for both SAX-3 “ligand” and “receptor” functions in RME circuit formation, while none of the Ig domains seems to be required.

Genetic Background	Transgene <i>Punc-33</i>	Phenotype (% Defect)		RME Analysis			Vab Head Analysis		
		RME	Vab Head	wt	sax-3	Rescue	wt	sax-3	Rescue
Control		0 ± 0	0 ± 0	/	***	ns	/	***	ns
sax-3		94 ± 1	25 ± 2.91	***	/	***	***	/	***
sax-3		8 ± 3.74	0 ± 0	ns	***	/	ns	***	/
sax-3		60 ± 3.09	3 ± 2.43	***	***	***	ns	*	ns
sax-3		21 ± 5.21	1 ± 0.67	ns	***	ns	ns	*	ns
sax-3		94 ± 1.76	29 ± 5.93	***	ns	***	***	ns	***
sax-3		60 ± 6.14	15 ± 1.33	***	***	***	***	ns	***
sax-3		41 ± 5.17	7 ± 0.67	***	***	***	***	*	***
sax-3		21 ± 0.67	0 ± 0	ns	***	ns	ns	***	ns
sax-3		11 ± 1.2	0 ± 0	ns	***	ns	ns	***	ns
sax-3		94 ± 1.76		***	ns	***			
sax-3		89 ± 4.37	9 ± 3.33	***	ns	***	ns	*	ns
sax-3		93 ± 0.58	24 ± 5.81	***	ns	***	***	ns	***

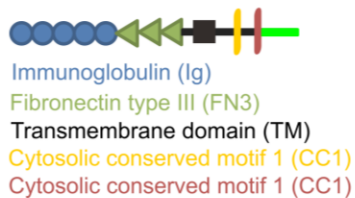

























Table. 1 Summarized Phenotyping Results of Rescuing Experiments with One Transgene

Transgenes are expressed in *ju1119* mutant background under a pan-neural promoter *Punc-33*. Phenotyping results are presented as mean and standard error of mean. Results from each genotype is compared to the grey boxed results in the “Rescue” section. Different degrees of Vab head phenotype are observed and all animals with the phenotype are categorized into “defected”. Statistical analysis: ns: no significance; *: $p < 0.05$; **: $p < 0.01$; ***: $p < 0.001$.

Transgene		Phenotype (% Defect)		RME Analysis		Vab Analysis	
<i>Punc-33</i>	<i>Punc-25</i>	RME	Vab Head	<i>sax-3</i>	Rescue	<i>sax-3</i>	Rescue
		94 ± 1	25 ± 2.91	/	***	/	***
		8 ± 3.74	0 ± 0	***	ns	***	ns
		92 ± 0	3 ± 1.33	ns	***	ns	***
		11 ± 2.67	0 ± 0	***	/	***	/
		52 ± 4	9 ± 1.76	***	***	*	*
		35 ± 3.33	6 ± 3.06	***	**	**	ns
		85 ± 3.71	13 ± 5.33	ns	***	ns	ns
		61 ± 5.93	1 ± 0.67	***	***	***	ns
		21 ± 2.9	5.33 ± 2.4	***	ns	***	ns
		98 ± 1.15	23 ± 5.93	ns	***	ns	***
		93 ± 0.58	24 ± 5.81	ns	***	ns	***
		15 ± 3.33	3 ± 0.67	***	ns	**	ns
		93 ± 0.58	23 ± 3.28	ns	***	ns	***
		67 ± 1.76	10 ± 2.19	***	***	**	*



Immunoglobulin (Ig)
 Fibronectin type III (FN3)
 Transmembrane domain (TM)
 Cytosolic conserved motif 1 (CC1)
 Cytosolic conserved motif 1 (CC1)

Table. 2 Summarized Phenotyping Results of Rescuing Experiments with Two Transgenes

Transgenes are expressed in *ju1119* mutant background under a pan-neural promoter *Punc-33* or a RME specific promoter *Punc-25*. Phenotyping results are presented as mean and standard error of mean. Results from each genotype is compared to the grey boxed genotype in the “Rescue” section. Different degrees of Vab head phenotype are observed and all animals with the phenotype are categorized into “defected”. Statistical analysis: ns: no significance; *: $p < 0.05$; **: $p < 0.01$; ***: $p < 0.001$.

Chapter 3. Conclusion and Future Directions

Studies in different organisms have shown that Robo is the receptor for the repulsive guidance cue Slit. Consistent with its function as a Slit receptor, loss-of-function in Robo causes many phenotypes that are shared by Slit mutants. However, close examination of Robo-related phenotypes also shows selective abnormal fasciculation of axons in *C. elegans*, *Drosophila*, Zebrafish, and cultured mammalian neurons, that are not related Slit. In *C. elegans*, there are only one Robo, SAX-3, and one Slit, slit-1. *sax-3(lf)* animals display many phenotypes that are not observed in Slit mutants, including embryonic lethality, abnormal head morphology (*vab*) and misplacement of neurons. Based on those observations, it has been long speculated the presence of Slit-independent regulation cross animal kingdom. While Slit -dependent and -independent homophilic and heterophilic interactions between Ig domains of different Robo isoforms have been shown *in vitro* and in cultured cells, the functional significance of such interactions is still unclear. Here, we present evidence to show that *C. elegans* Robo/SAX-3 can be cleaved at the extracellular FN3 repeats and intracellular domains in a developmental stage specific manner. The intracellular cleavage of SAX-3/Robo happens at the same time with the extracellular cleavage and could depend on the extracellular cleavage like Netrin receptors. The intracellular cleavage fragment is predominantly located in the nucleus, and its nuclear localization is also Slit-independent. We also show that

the extracellular region of SAX-3/Robo is sufficient to regulate embryonic development and head morphogenesis, which further supports its non-receptor functions. As similar embryonic lethality and abnormal head morphology phenotypes are observed in many ECM mutants, these results also suggest that SAX-3 may function as a critical organizer or component of ECM. The function of SAX-3/Robo in neuronal development requires the extracellular regulation, the intracellular cleavage and the nuclear translocation of SAX-3 C-terminus.

The extracellular domains of Robo receptors are evolutionally conserved from nematodes to mammals and share high levels of homology to other CAMs such as NCAM and DCC. As shown in many CAMs, it is not surprising that the Robo can form homophilic interactions through their extracellular domains. However, most of reported homophilic interactions of CAMs including Robo are through Ig domains. FN3 repeats have been considered mostly as a structural domain, and their active biological functions have not been well characterized. Here we present evidence that FN3 repeats are essential for the Slit-independent Robo regulation and are required for the cleavage of SAX-3 in both extracellular and intracellular domains.

The intracellular region of Robo receptors is clearly different to any of other CAMs. First, unlike the extracellular domains, the intracellular region of Robo receptors is not evolutionarily conserved. Little conservation in this region is found among nematodes, flies and mammals. There are several conserved

stretches of amino acids, conserved cytoplasmic motifs (CC), in the intracellular region. However, the degree of conservation among different species is not impressive. Second, the intracellular region of Robo receptors doesn't have any identifiable domains or predicated catalytic activity. Sequence analysis of the intracellular region of Robo receptors doesn't yield any potential secondary structure either. It appears that the intracellular region of Robo receptors is a long intrinsically unstructured polypeptide. Through genetic and biochemical studies, many proteins have been identified to interact with the intracellular region of Robo receptors, including small GTPase, PI3 kinase, WAVE complex and other CAMs, and most of those interactions are conserved from nematodes to mammals. It is still unclear that with the unconserved and unstructured nature of the intracellular region, how Robo receptors interact with similar binding partners in different organisms. Here we show that the intracellular region of SAX-3/Robo can be cleaved at specific developmental stages, and the cleavage product translocates into the nucleus. Unlike other downstream signals, this cleavage is not dependent on Slit. The essential role of the nuclear localization of the cleaved fragment also suggests that it may be involved in transcriptional regulations.

References

1. Seeger, M., et al., *Mutations affecting growth cone guidance in Drosophila: genes necessary for guidance toward or away from the midline*. Neuron, 1993. **10**(3): p. 409-26.
2. Zallen, J.A., S.A. Kirch, and C.I. Bargmann, *Genes required for axon pathfinding and extension in the C. elegans nerve ring*. Development, 1999. **126**(16): p. 3679-92.
3. Dickson, B.J. and G.F. Gilestro, *Regulation of commissural axon pathfinding by slit and its Robo receptors*. Annu Rev Cell Dev Biol, 2006. **22**: p. 651-75.
4. Park, K.W., et al., *Robo4 is a vascular-specific receptor that inhibits endothelial migration*. Dev Biol, 2003. **261**(1): p. 251-67.
5. Brose, K., et al., *Slit proteins bind Robo receptors and have an evolutionarily conserved role in repulsive axon guidance*. Cell, 1999. **96**(6): p. 795-806.
6. Kidd, T., K.S. Bland, and C.S. Goodman, *Slit is the midline repellent for the robo receptor in Drosophila*. Cell, 1999. **96**(6): p. 785-94.
7. Rothberg, J.M., et al., *slit: an extracellular protein necessary for development of midline glia and commissural axon pathways contains both EGF and LRR domains*. Genes Dev, 1990. **4**(12A): p. 2169-87.
8. Brose, K. and M. Tessier-Lavigne, *Slit proteins: key regulators of axon guidance, axonal branching, and cell migration*. Curr Opin Neurobiol, 2000. **10**(1): p. 95-102.
9. Morlot, C., et al., *Structural insights into the Slit-Robo complex*. Proc Natl Acad Sci U S A, 2007. **104**(38): p. 14923-8.
10. Delloye-Bourgeois, C., et al., *PlexinA1 is a new Slit receptor and mediates axon guidance function of Slit C-terminal fragments*. Nat Neurosci, 2015. **18**(1): p. 36-45.
11. Wong, K., et al., *Signal transduction in neuronal migration: roles of GTPase activating proteins and the small GTPase Cdc42 in the Slit-Robo pathway*. Cell, 2001. **107**(2): p. 209-21.
12. Li, X., et al., *Structural basis of Robo proline-rich motif recognition by the srGAP1 Src homology 3 domain in the Slit-Robo signaling pathway*. J Biol Chem, 2006. **281**(38): p. 28430-7.

13. Bacon, C., V. Endris, and G. Rappold, *Dynamic expression of the Slit-Robo GTPase activating protein genes during development of the murine nervous system*. J Comp Neurol, 2009. **513**(2): p. 224-36.
14. Endris, V., et al., *The novel Rho-GTPase activating gene MEGAP/ srGAP3 has a putative role in severe mental retardation*. Proc Natl Acad Sci U S A, 2002. **99**(18): p. 11754-9.
15. Lundstrom, A., et al., *Vilse, a conserved Rac/Cdc42 GAP mediating Robo repulsion in tracheal cells and axons*. Genes Dev, 2004. **18**(17): p. 2161-71.
16. Wills, Z., et al., *The tyrosine kinase Abl and its substrate enabled collaborate with the receptor phosphatase Dlar to control motor axon guidance*. Neuron, 1999. **22**(2): p. 301-12.
17. Bashaw, G.J., et al., *Repulsive axon guidance: Abelson and Enabled play opposing roles downstream of the roundabout receptor*. Cell, 2000. **101**(7): p. 703-15.
18. Rhee, J., et al., *Activation of the repulsive receptor Roundabout inhibits N-cadherin-mediated cell adhesion*. Nat Cell Biol, 2002. **4**(10): p. 798-805.
19. Rhee, J., et al., *Cables links Robo-bound Abl kinase to N-cadherin-bound beta-catenin to mediate Slit-induced modulation of adhesion and transcription*. Nat Cell Biol, 2007. **9**(8): p. 883-92.
20. Sabatier, C., et al., *The divergent Robo family protein rig-1/Robo3 is a negative regulator of slit responsiveness required for midline crossing by commissural axons*. Cell, 2004. **117**(2): p. 157-69.
21. Friocourt, F. and A. Chedotal, *The Robo3 receptor, a key player in the development, evolution, and function of commissural systems*. Dev Neurobiol, 2017. **77**(7): p. 876-890.
22. Zelina, P., et al., *Signaling switch of the axon guidance receptor Robo3 during vertebrate evolution*. Neuron, 2014. **84**(6): p. 1258-72.
23. Chen, Z., et al., *Alternative splicing of the Robo3 axon guidance receptor governs the midline switch from attraction to repulsion*. Neuron, 2008. **58**(3): p. 325-32.
24. Borrell, V., et al., *Slit/Robo signaling modulates the proliferation of central nervous system progenitors*. Neuron, 2012. **76**(2): p. 338-52.
25. Fricke, C., et al., *astray, a zebrafish roundabout homolog required for retinal axon guidance*. Science, 2001. **292**(5516): p. 507-10.

26. Piper, M., et al., *Signaling mechanisms underlying Slit2-induced collapse of Xenopus retinal growth cones*. Neuron, 2006. **49**(2): p. 215-28.
27. Long, H., et al., *Conserved roles for Slit and Robo proteins in midline commissural axon guidance*. Neuron, 2004. **42**(2): p. 213-23.
28. Jen, J.C., et al., *Mutations in a human ROBO gene disrupt hindbrain axon pathway crossing and morphogenesis*. Science, 2004. **304**(5676): p. 1509-13.
29. Jaworski, A. and M. Tessier-Lavigne, *Autocrine/juxtacrine regulation of axon fasciculation by Slit-Robo signaling*. Nat Neurosci, 2012. **15**(3): p. 367-9.
30. Bhat, K.M., *Post-guidance signaling by extracellular matrix-associated Slit/Slit-N maintains fasciculation and position of axon tracts in the nerve cord*. PLoS Genet, 2017. **13**(11): p. e1007094.
31. Hu, H., *Chemorepulsion of neuronal migration by Slit2 in the developing mammalian forebrain*. Neuron, 1999. **23**(4): p. 703-11.
32. Bjorke, B., et al., *Contralateral migration of oculomotor neurons is regulated by Slit/Robo signaling*. Neural Dev, 2016. **11**(1): p. 18.
33. Whitford, K.L., et al., *Regulation of cortical dendrite development by Slit-Robo interactions*. Neuron, 2002. **33**(1): p. 47-61.
34. Grieshammer, U., et al., *SLIT2-mediated ROBO2 signaling restricts kidney induction to a single site*. Dev Cell, 2004. **6**(5): p. 709-17.
35. Domyan, E.T., et al., *Roundabout receptors are critical for foregut separation from the body wall*. Dev Cell, 2013. **24**(1): p. 52-63.
36. Santiago-Martinez, E., N.H. Soplan, and S.G. Kramer, *Lateral positioning at the dorsal midline: Slit and Roundabout receptors guide Drosophila heart cell migration*. Proc Natl Acad Sci U S A, 2006. **103**(33): p. 12441-6.
37. Amodeo, V., et al., *A PML/Slit Axis Controls Physiological Cell Migration and Cancer Invasion in the CNS*. Cell Rep, 2017. **20**(2): p. 411-426.
38. Biteau, B. and H. Jasper, *Slit/Robo signaling regulates cell fate decisions in the intestinal stem cell lineage of Drosophila*. Cell Rep, 2014. **7**(6): p. 1867-75.
39. Yang, Y.H., et al., *Intra-islet SLIT-ROBO signaling is required for beta-cell survival and potentiates insulin secretion*. Proc Natl Acad Sci U S A, 2013. **110**(41): p. 16480-5.

40. Wang, B., et al., *Induction of tumor angiogenesis by Slit-Robo signaling and inhibition of cancer growth by blocking Robo activity*. *Cancer Cell*, 2003. **4**(1): p. 19-29.
41. Liu, Z.J. and M. Herlyn, *Slit-Robo: neuronal guides signal in tumor angiogenesis*. *Cancer Cell*, 2003. **4**(1): p. 1-2.
42. Yang, X.M., et al., *Slit-Robo signaling mediates lymphangiogenesis and promotes tumor lymphatic metastasis*. *Biochem Biophys Res Commun*, 2010. **396**(2): p. 571-7.
43. Dickinson, R.E., et al., *Glucocorticoid regulation of SLIT/ROBO tumour suppressor genes in the ovarian surface epithelium and ovarian cancer cells*. *PLoS One*, 2011. **6**(11): p. e27792.
44. Parsons, L., et al., *Roundabout gene family functions during sensory axon guidance in the drosophila embryo are mediated by both Slit-dependent and Slit-independent mechanisms*. *Dev Biol*, 2003. **264**(2): p. 363-75.
45. Andrews, W.D., M. Barber, and J.G. Parnavelas, *Slit-Robo interactions during cortical development*. *J Anat*, 2007. **211**(2): p. 188-98.
46. Jaworski, A., et al., *Operational redundancy in axon guidance through the multifunctional receptor Robo3 and its ligand NELL2*. *Science*, 2015. **350**(6263): p. 961-5.
47. Rao, Y., X. Zhao, and C.H. Siu, *Mechanism of homophilic binding mediated by the neural cell adhesion molecule NCAM. Evidence for isologous interaction*. *J Biol Chem*, 1994. **269**(44): p. 27540-8.
48. Yip, P.M. and C.H. Siu, *PC12 cells utilize the homophilic binding site of L1 for cell-cell adhesion but L1-alpha v beta 3 interaction for neurite outgrowth*. *J Neurochem*, 2001. **76**(5): p. 1552-64.
49. Hivert, B., et al., *Robo1 and Robo2 are homophilic binding molecules that promote axonal growth*. *Mol Cell Neurosci*, 2002. **21**(4): p. 534-45.
50. Camurri, L., et al., *Evidence for the existence of two Robo3 isoforms with divergent biochemical properties*. *Mol Cell Neurosci*, 2005. **30**(4): p. 485-93.
51. Hao, J.C., et al., *C-elegans slit acts in midline, dorsal-ventral, and anterior-posterior guidance via the SAX-3/Robo receptor*. *Neuron*, 2001. **32**(1): p. 25-38.
52. Berg, J.M., J.L. Tymoczko, and L. Stryer, *Biochemistry, Fifth Edition*. 2002: W.H. Freeman.

53. Hattori, M., M. Osterfield, and J.G. Flanagan, *Regulated cleavage of a contact-mediated axon repellent*. *Science*, 2000. **289**(5483): p. 1360-5.
54. Bai, G., et al., *Presenilin-dependent receptor processing is required for axon guidance*. *Cell*, 2011. **144**(1): p. 106-18.
55. Taniguchi, Y., S.H. Kim, and S.S. Sisodia, *Presenilin-dependent "gamma-secretase" processing of deleted in colorectal cancer (DCC)*. *J Biol Chem*, 2003. **278**(33): p. 30425-8.
56. Neuhaus-Follini, A. and G.J. Bashaw, *The Intracellular Domain of the Frazzled/DCC Receptor Is a Transcription Factor Required for Commissural Axon Guidance*. *Neuron*, 2015. **87**(4): p. 751-63.
57. Coleman, H.A., et al., *The Adam family metalloprotease Kuzbanian regulates the cleavage of the roundabout receptor to control axon repulsion at the midline*. *Development*, 2010. **137**(14): p. 2417-26.